AENSI Journals

Australian Journal of Basic and Applied Sciences

ISSN:1991-8178

Journal home page: www.ajbasweb.com

Analysis of the Active Region of Archimedean Spiral Antenna

[1]Abdirahman Mohamoud Shire and [2]Fauziahanim Che Seman

Wireless and Radio Science Centre (WARAS) Faculty of Electrical and Electronic Engineering University Tun Hussein Onn Malaysia 86400 Parit Raja, Johor Malaysia.

ARTICLE INFO

Article history:
Received 25 April 2014
Received in revised form
8 May 2014
Accepted 20 May 2014
Available online 17 June 2014

Key words:

ABSTRACT

he paper elaborates the current distribution of the Archimedean Spiral Antenna (ASA), demonstrating the concept of frequency dependent active region and this determines the effective radiation area on the spiral arm. The band theory is used to explain the theoretical principles of the operation of the spiral antenna. In this paper, a two arm Archimedean spiral antenna is designed using Computer Simulation Technology, (CST). The properties of the active region of the spiral antenna are analyzed in different types of dielectric substrates. The calculated and simulations results show the position of the active region is very dependent to the operating frequency and dielectric permittivity of the substrates. The maximum surface current induced to the spiral arm increases as the operating frequency and permittivity of the dielectric substrates reduces.

To Cite This Article: Abdirahman Mohamoud Shire and Fauziahanim Che Seman., Analysis of the Active Region of Archimedean Spiral Antenna. ***Aust. J. Basic & Appl. Sci.,*** *8(21): 12-17, 2014*

INTRODUCTION

Frequency independent antennas currently receive huge interest (Dyson, J.D., 1962; Jordan, E.C., et al., 1964) due to their special properties in wideband applications. The term frequency-independent (FI) is reserved for antennas with electrical characteristics that vary insignificantly over an extremely wide operating frequency range (McFadden, M., 2009). This properties is valid on its own and an improper insertion of the ground plane (GP) behind the antenna might distrupt the FI belonginess (Nakano, H. and K. Nogami, 2007). In this paper, the key important parameters of the FI of an Archimedean Spiral Antenna backed by a metalic plate has been analysed accordingly. In ASA the FI property is contributed by the position of the active region on the spiral arm where the effective radiation pattern of the ASA take places. Then the GP is carefully inserted in order to provide a unidirectional radiation pattern and a higher gain (Shire, A.M. and F.C. Seman, 2012) and later, the possible change of the active region indicated by the current distribution on the spiral arm is analysed. Furthermore, the variation of the magnitude of the current induced to the spiral arm with operating frequency range and dielectric substrates is investigated.

The organization of the paper is described as follows; in the theoretical operation section of the ASA, the current distribution along the spiral arm is analyzed numerically. Later, the maximum current induced on the spiral arm associated by the position of the active region is analyzed based on the numerical and the simulation results.

Theoretical Operation for Spiral Antenna:

Considering a two-arm spiral antenna operating in Mode 1, which is fed from its center at ports X and X' as illustrated in Fig. 1. The band theory (radiating ring theory) is applied to explain the theoretical principles behind the operation of the antenna. The current distribution on the antenna is divided in to three areas, which are feeding region, transition region and decay region (Yeh, Y.S. and K.K. Mei, 1964).

Corresponding Author: Abdirahman Mohamoud Shire, Wireless and Radio Science Centre (WARAS) Faculty of Electrical and Electronic Engineering University Tun Hussein Onn Malaysia 86400 Parit Raja, Johor Malaysia.
E-mail: shire_288@hotmail.com

Australian Journal of Basic and Applied Sciences, 8(21) Special 2014, Pages: 12-17

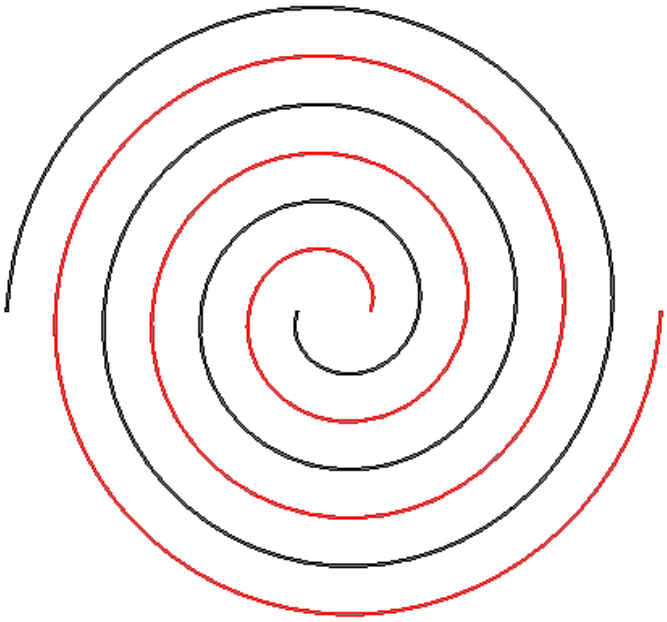

Fig. 1: Active region of spiral antenna based on Radiation band theory

The spiral antenna is fed at $\bar{r}+(0)$ and $\bar{r}-(0)$, which presents the time harmonic excitation of the spiral. Then, the current at the point $\bar{r}\pm(\theta)$ and the phase of the current on the spiral antenna is expressed by the travel time from the feeding is defined in equation (1) and (2) respectively [37 and 8]:

$$I_{\pm}(\theta,t)=i_{\pm}(\theta)\, e^{j\omega t}. \quad (1)$$

"t" _"d" "=" ("s" _"±" "(θ)")/"v" _"p" . (2)

Where the real current of the spiral is the real part of $I\pm(\theta, t)$, $i\pm(\theta)$ is a complex of θ, vp is the phase velocity and $s\pm(\theta)$ is the distance along the spiral arms and it is found as :

$$s_{\pm}(\theta)-s_{\pm}(\theta)=\int_0^{\theta}\left|\left(\left[\left[d\bar{r}\right]\right]_{\pm}(\theta)\right)/d\theta\right|\, d\theta=\int_0^{\theta}\left[\left[\sqrt{((dr(\theta)/d\theta)^{2}+(r\, d\theta/d\theta)}d\theta\right)\right]\right.= (e^{a\theta}-1)\ \sqrt{(1+1/a^{2})}\left.\right]. \quad (3)$$

The phase of the current is

$$\angle I_{\pm}(\theta,t)=\angle I_{\pm}(\theta,t-t_d)=\angle I_{\pm}(\theta)\, e^{j\omega t}+\angle e^{(-j\omega t)}$$
$$=\angle I_{\pm}(\theta,t)-(2\pi f\, s\pm(\theta))/v_p =\angle I_{\pm}(\theta,t)-(2\pi f\, s\pm(\theta))/\lambda. \quad (4)$$

In the Feeding region, the spiral antenna is fed in a balanced feeding at points X and X' as illustrated in Fig.1, and the feeding diameter is very small compared to the wavelength, due to that, the current these points are anti-phase and it is calculated as:

$$\angle I_{+}(\pi,t)-\angle I_{-}(0,t)\approx\angle I_{+}(0,t)-\angle I_{+}(\pi,t)=\pi. \quad (5)$$

The simplified mathematical formulation of active region of spiral antenna is analyzed and presented:

$$r(\theta)=e^{(a\theta+b)}. \quad (6)$$

The spiral arm rotates accordingly which can be represented as a curve (Rumsey, V.H., 1957; Kaiser, J.A., 1960) and in polar coordinate, the constants a determines the rate of wrapping and scales the curve, constant b scales the curve, while θ is angle of the phase and calculated as:

$$\theta=1/a\ \log(\lambda/(2(e^{a\pi}-1)\ \sqrt{(1+a^{(-2)}}))). \quad (7)$$

Spiral with tight wrapping can facilitate to describe the active region in simple way, so letting b tend to zero; it is obtained an approximate radiation condition from equations (6) and (7):

Australian Journal of Basic and Applied Sciences, 8(21) Special 2014, Pages: 12-17

$$r(\theta)=e^{a\theta}=a\lambda/(2(-1+e^{a\pi})\sqrt{(1+a^2)})\approx a\lambda/2(-1+1+a\pi+\cdots)1\approx\lambda/((2\pi)), 2\pi r(\theta)=\lambda. \quad (8)$$

Based on "radiation band" theory, equation (8) clearly elaborates the Mode 1 radiation predominantly occurs from the area whose circumference is approximately one of wavelength (C=1λ) (Kaiser, J.A., 1960; Bawer, R. and J.J. Wolfe, 1955; Burdine, B.H.,) as indicated in Fig.1 at points Y and Y', which belong to neigbouring arms, because the current flowing in contiguous arms is in phase leading to coherent or constructive radiation in the far-field. On the other side, the same conditions occured diametrically opposite points Z and Z'. This area defines the position of the active region, where most of the radiation takes place due to the decaying of the in-phase current.

Outside these regions the current is not in- phase and, therefore, the radiated field interferes destructively (Kaiser, J.A., 1960; Bawer, R. and J.J. Wolfe, 1955; Burdine, B.H.,). The nonradiated traveling wave currents will flow past this region, and if the size of the spiral permits, radiate in the next properly phased section in which the in-phase current conditions will show up at odd wavelength circumferences of the spiral and higher order modes will radiate (this will occur at a circumference equal to three wavelengths; mode 3 for a two-arm spiral). If the spiral is not large enough, the currents will reach the end of the spiral arms where they are either absorbed or reflected back toward the spiral's center.The position of the active region vary accordingly with the changes of the dielectric permittivity as defined by Equation (9).

$$r\_eff=\lambda\_eff/2\pi=\lambda\_0/(2\pi\sqrt{(\varepsilon\_eff)}). \quad (9)$$

Archimedean Spiral Antenna Design:

The ASA is designed using CST MWS where the operating frequency range is chosen to be in the 2-12GHz range and this frequency range is available for UWB applications. The arm width (w), arm spacing (s), inner radius (r1) and the outer radius (r2) of the ASA are calculated using equations in (Shire, A.M. and F.C. Seman, 2012). The r2 is optimized to be 35 mm while the other parameters are optimized to be 1.3 mm. The number of turns of each arm is selected as 8 turns and in computer model, the ASA is fed at the center using discrete port. The spiral arm is cascaded to an electrically □ /4 thick dielectric substrate backing by a metallic plate.

Results and Analysis:

Fig.1 shows the current distribution on the spiral arm in which indicating the current behavior in the feeding region, transition region and decay region. In the feeding region, the current at neighbor arms is anti-phase as proven in Equation (5) thus there is no radiation takes place and this is illustrated in Fig.1 (a). The calculated phase at Equation (5) is 1800, so since the phase difference at points X and X' is 1800 out phase, the radiation is negligible because the two current waves of the two neighbor arms are cancelling each other due to the anti-phase condition. According to the current distribution theory of spiral antenna, the current reaches its maximum at the end of the feeding region which is clearly observed in the simulated current on the spiral antenna, in which the maximum current magnitude is 82.57 A/m. The current starts to decay to 69.24 A/m at the transition region as shown in Fig.2 (b), but still no effective radiation takes place in this region since the currents at the neighbor arms are anti-phase.

Identification of the position of the active region in decay region is done based on the (i) calculation (See Table 1, third column) by referring to Equation (8) and (ii) current distribution of the CST simulation results (Refer to Table 1, fourth column). Note that the spiral arm is attached on the free space so the dielectric permittivity, □ r is 1. Fig.1shows that at the lower operating frequency, the active region of the spiral is located around the perimeter (see Fig.2 (a)) of the antenna and as the frequency increases the position of the active region moves inwards the center feeding (see Fig. 2 (c)). The simulated active regions of the active region are shown in Fig.2. The calculated and simulated locations of the active region are tabulated in Table 1 and the comparisons of the two results are shown in Fig.3.

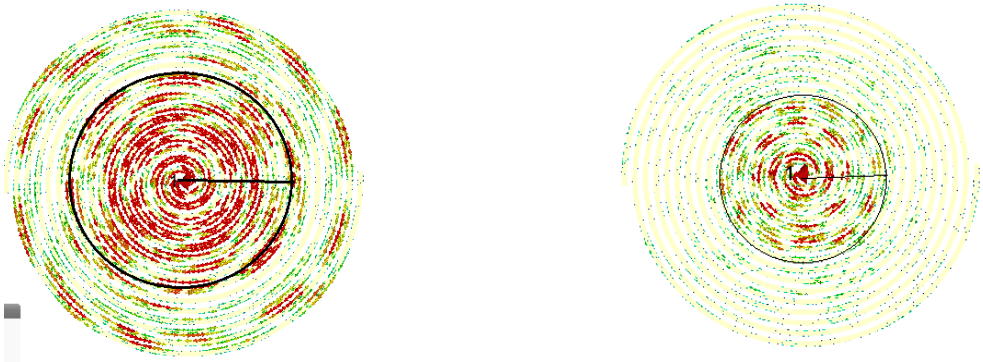

Australian Journal of Basic and Applied Sciences, 8(21) Special 2014, Pages: 12-17

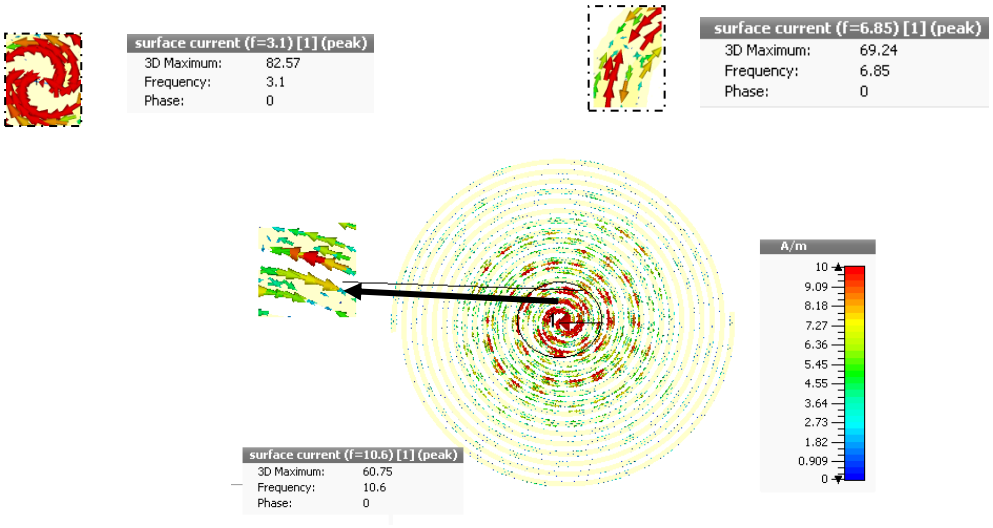

Fig. 2: Current distribution of two arms Archimedean spiral antenna is shown as black band for different frequencies (a) 3.1GHz, (b) 6.85GHz and (c) 10.6GHz

Table 1: Details position of the active region

Frequency (GHz)	λ (mm)	$r(\theta)$ (mm) Calculation	$r(\theta)$ (mm) Simulation
2	150	23.87	25
3	100	15.92	16
4	75	11.94	12.5
5	60	9.4	9.5
6	50	7.96	8.2
7	42.86	6.82	8
8	37.5	5.96	7.5
9	33.33	5.31	6
10	30	4.78	5.5
11	27.27	4.34	4.8
12	*25*	3.98	4

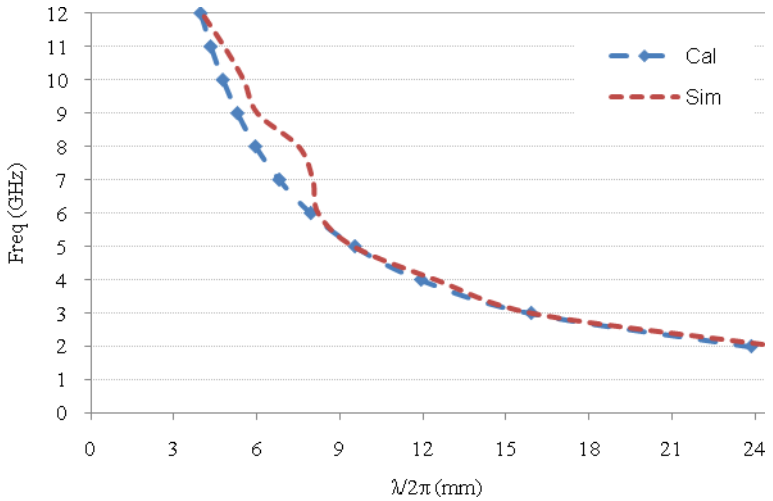

Fig. 3: Calculation and simulation results of position of the active region of ASA

Table 2: The maximum current distribution (A/m) at the active region

Frequency (GHz)	λ (mm)	$r(\theta)$ (mm) Calculation	$r(\theta)$ (mm) Simulation
1	82.57A/m	69.24A/m	60.75A/m
2.33	70.41A/m	62.38A/m	56.3A/m
4.3	65.75A/m	57.83A/m	52.93A/m
10.2	57.39A/m	53.21A/m	49.51A/m

The ASA spiral antenna is simulated on four different substrates permittivity, □ r in order to examine the effect of the dielectric substrate on the characteristics of the active region of the ASA. It is clearly seen in Table 2 that as □ r increases from 1 to 2.33, the maximum current induced at the active region reduces from 82.57A/m to 70.41 A/m. The maximum current reduces 12.7% as □ r increases from 4.3 to 10.2. This is due as the currents propagate along the spiral arm, a higher dielectric permittivity assimilates more input power fed to the antenna and therefore leads to reduction of the current distribution on the spiral arms (Burdine, B.H.). The current magnitude also degrades as the operating frequency of the ASA increases because spiral antenna behaves like inductive circuit at higher frequencies, so the impedance of the inductive circuit increases as the frequency increases which leads to the reduction of the current magnitude (Rosu, I.,).

The location of the active region of the ASA changes as the dielectric permittivity increases from 1 to 10.2. Numerically, based on Equation (9), as the substrate permittivity increases, the location of the active region shrinks towards the center feeding of the ASA. This is proven at the operating frequency of 2 GHz when εr =2.33 the active region is positioned 18.5 mm from the center fed and this significantly reduces 10.1 mm when εr =10.2 as demonstrated in Fig. 4.As the operating frequency increases to 12 GHz, the position of the active region occurs 1.68 mm and 3.08 mm away from the feeding point for εr =10.2 and εr =2.33 respectively. Again, the higher dielectric substrate slows the traveling wave in which leads to shrinkage of the active region area and increases the coupling between the neighboring arms (Shire, A.M. and F.C. Seman, 2012). Both calculation and simulation results demonstrates excellent agreement as shown in Fig. 4.

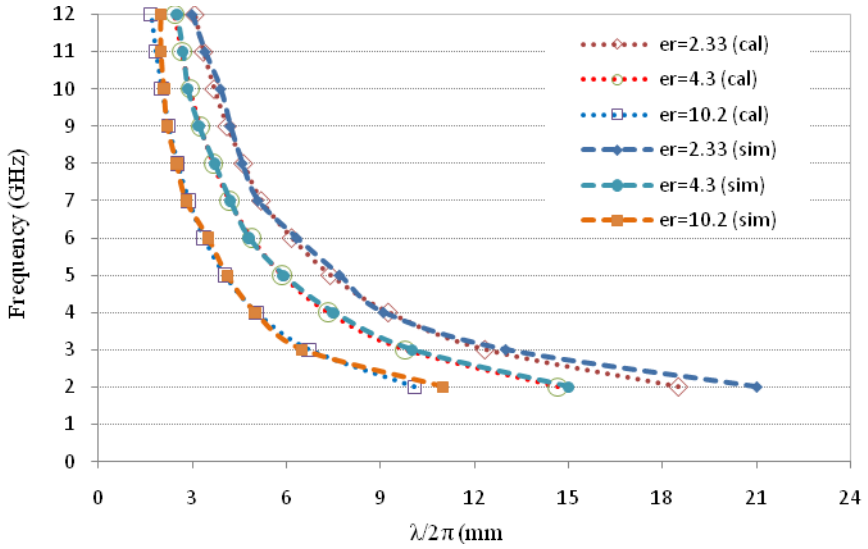

Fig. 4: Calculated and simulated results of the position of the active region of ASA on different dielectric substrate

Conclusion:

The characteristics of the active region based calculation and simulation results are presented in this paper. The ASA is designed in CST to operate between 2 and 12GHz for UWB applications. It demonstrated that the position of the active region depends on both operating frequency and dielectric substrate. As the operating frequency and the substrate permittivity increases, the locality of the active region shrinks inward the antenna.

REFERENCES

Burdine, B.H., "The spiral antenna," Massachusetts Institute of Technology, Research Laboratory Technical Report, Tech. Rep.

Bawer, R. and J.J. Wolfe, 1955."The spiral antenna," I.R.E. International Convention Record, March 1960.

Dyson, J.D., 1962. "Frequency-independent antennas" Survey of development, Electronics, 1-01 35, pp: 39-44.

Jordan, E.C., G.A. Deschamps, J.D. Dyson and P.E. Mayes, 1964. "Developments in broadband antennas, ZEEE Spectrum, 1: 58-71.

Kaiser, J.A., 1960. "the Archimedean two-wire spiral antenna" IRET Transactions on Antennas and Propagation, AP-8: 312-323.

McFadden, M., 2009. "Analysis of Equiangular Spiral Antenna" PhD Dissertation, Georgia Institute of Technology.

Nakano, H. and K. Nogami, 2007. "A spiral antenna backed by a conducting plane reflector," IEEE Trans. Antennas Propag., AP-34: 1417–1423.

Rosu, I., "Microstrip, Strip Line and CPW Design" RF Technical Artical, http://www.qsl.net/va3iul

Rumsey, V.H., 1957. "Frequency independent antennas," IRE National Convention Record, 5: 114-118.

Shire, A.M. and F.C. Seman, 2012. " Effects of dielectric substrate on the performance of UWB Archimedean spiral antenna" Proceeding of the 2013 IEEE International Conference on Space Science and Communication (IconSpace), pp: 412-415.

Yeh, Y.S. and K.K. Mei, 1964." Theory of Conical Equiangular Spiral Antennas, Part II- Current Distributions and Input Impedances" IEEE Transactions on Antennas and Propagation, 16: 14-21.